



Chakraborty, M., Nikbakhtnasrabadi, F. and Dahiya, R. (2022) Hybrid integration of screen-printed RFID tags and rigid microchip on paper. *IEEE Journal on Flexible Electronics*, (doi: 10.1109/JFLEX.2022.3165515).

There may be differences between this version and the published version. You are advised to consult the publisher's version if you wish to cite from it.

<https://eprints.gla.ac.uk/268392/>

Deposited on: 1 April 2022

Enlighten – Research publications by members of the University of Glasgow  
<https://eprints.gla.ac.uk>

# Hybrid Integration of Screen-Printed Smart RFID Tags with Rigid Microchip

Moupali Chakraborty\*, *Member IEEE*, Fatemeh Nikbakhtnasrabadi\*, *Student Member IEEE*, and Ravinder Dahiya, *Fellow, IEEE*  
(\*Equal contribution)

Bendable Electronics and Sensing Technologies (BEST) Group,  
James Watt School of Engineering, University of Glasgow, G12 8QQ, UK  
Correspondence to: [Ravinder.Dahiya@glasgow.ac.uk](mailto:Ravinder.Dahiya@glasgow.ac.uk)

**Abstract**— Hybrid or heterogenous integration of silicon technologies and printed electronics is a promising approach for high-performance flexible electronics. It is essentially the integration of rigid microchips with the printed circuit on a flexible substrate. However, microchips with no-lead and mm size pitch introduce practical challenges in terms of precise electrical bonding onto the printed pattern. The differences in mechanical and thermal requirements also make it challenging to use conventional bonding and interconnect technology to robustly connect the microchips on flexible substrates. The focus of this work is to present these challenges with respect to different substrate-adhesive combinations and to provide a facile technique for integrating NFC microchips on different flexible substrates. Following the successful integration, the smart tags were characterised to demonstrate reliable performance in the NFC reading range. Whilst presenting a hybrid integration for the smart tag, this work also shows a potential solution for several other applications of flexible electronics where high-performance cannot be achieved by printed electronics alone.

**Keywords**—Flexible electronics; printed electronics; Smart Tag; Heterogenous Integration; Electrical bonding; Hybrid integration

## I. INTRODUCTION

Hybrid or heterogenous flexible electronic systems that combine silicon technology and printed electronics are promising approaches due to benefits such as high-performance (of silicon technology) and low-cost resource-efficient fabrication (of printed electronics) [1]. These attributes are needed to extend the effective use of flexible electronics in applications such as smart tags, internet of things (IoT) wearables, robotics, ultra-thin displays, healthcare, etc. [2]. It is difficult to have these attributes with current silicon technology or printed electronics alone and putting together the devices as hybrid systems is a practical way forward. The approach could add significant value to smart radio frequency identification (RFID) tags or labels, which are in high demand as they could enhance visibility and efficiency across the supply chain and brand differentiation in a variety of industries [3, 4]. However, they are mainly passive or chipless. Among others, the difficulties related to the integration of chips make it challenging to develop active tags.

Different printed electronics technologies such as screen printing, inkjet printing, roll-to-roll printing, nanoimprint etc. have been explored for realising the passive components such as conductive tracks to realise the smart tag antenna on various substrates [5-8]. The off-the-shelf rigid microchips can then be integrated with these printed passive components

to develop smart tags for various applications. The common practice is to mount the microchip and high-performing SMT (Surface Mounting Technology) components on the dedicated printed pads that are connected to printed tracks of the tag. However, the small size of the pads (here, 0.25 mm) makes it challenging to mount the chips on printed tracks as the spreading of ink may lead to short-circuiting. This is even more challenging for applications such as wearable systems, food packages, etc. [9-12], where smart tags are needed in flexible form factors and hence microchips need to be integrated on non-conventional substrates such as polymers and papers. In addition, difficulties in terms of stable adhesion of electronic components on flexible substrates make it challenging to obtain reliable electrical contacts [13].

In our previous works, we demonstrated the smart RFID tag for health and food quality monitoring [9, 11] by first integrating NFC (Near-Field-Communication) chip and antenna on a rigid FR-4 substrate (for real-time monitoring of temperature and strain) and then on flexible polyimide substrate. This followed the integration strategies used for mounting off-the-shelf rigid electronic components on flexible printed circuits boards (PCBs) [14]. However, both the rigid and flexible tags developed earlier, followed the conventional copper etching method used for standard PCBs. However, this approach does not take advantage of the direct printing of conductive tracks on flexible substrates. Further, this approach also leads to the generation of electronic waste (e-waste) due to the unused etched copper. This could be overcome by the resource-efficient additive manufacturing (AM) route, which has been used to develop different types of NFC smart tags and printed circuits boards [15-20]. This approach commonly uses Thin Shrink Small Outline Package (TSSOP) for the electrical bonding of NFC chips. However, electrical bonding of the SMT Integrated Circuits (ICs), resistors, capacitors are still challenging as the mechanical stability of the adhered components is not comparable with the rigid and flexible copper-etched tags. Interestingly, no literature has described the challenges for mounting the VQFN (Very thin Quad-Flat No-leads) packaged SMT components on the screen-printed tags. Furthermore, most of the substrate materials currently used in printed tags are not biodegradable. The work presented in this paper addresses this gap by demonstrating robust electrical bonding with the stable mechanical attachment of the SMT components, leading to flexible smart tags with ‘Green Hybrid Electronics’. In this regard, we present in detail the experimental studies showing the practical challenges of bonding VQFN packaged NFC transponder on the screen-printed conductive Ag (silver) track. Thereafter, the fully functionalised printed smart tag is characterized by varying

the antenna structure. Through the development of smart tags on paper, this work also shows a path towards hybrid integration of electronics on non-conventional flexible substrates.

This paper is organised as follows: The design, simulation, and fabrication of smart tags are explained in Section II. This is followed by the presentation of practical difficulties related to electrical bonding and mechanical stability in Section III. The solution explored here to overcome these practical difficulties is described in Section IV and the characterisation results for the developed smart tag are presented in Section V. Finally, a summary of key outcomes is given in Section VI.

## II. DESIGN OF TAG

### A. Materials and Components

Based on the NFC protocols the resonance frequency of a parallel inductor and capacitor is 13.56 MHz [9, 11]. A near field tag consists of an antenna which is an inductive coil of inductance  $L$ , an electronic chip that performs the communication operations as well as contains the tag identifier, and finally a capacitance  $C$  which is used to adjust the resonance frequency of the tag LC circuit [21]. The NFC transponder chosen for this work is RF430FRL152H, a programmable 16-bit MSP430 low-power microcontroller-based integrated circuit (IC) from Texas Instruments (Dallas, Texas, USA), that includes an internal capacitor ( $C_{int}$ ) of 35 pF. According to equation (1) to achieve resonance at the frequency of interest we have chosen an external capacitor

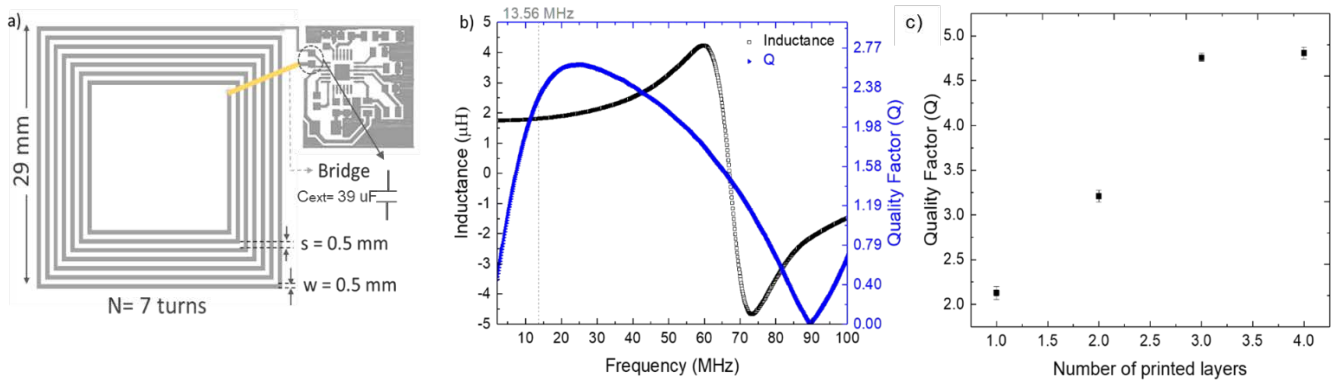


**Fig. 1.** (a) Layout of the printed inductor and circuit part. (b) Inductance and quality factor of the printed inductor before connecting an RF IC chip. (c) Effect of the number of printed layers on the quality factor.

**TABLE I:** SIMULATION (SIM.) AND MEASURED (MEAS.) VALUES FOR THE INDUCTORS WITH THEIR GEOMETRIES

Design No.	No. of Turns	Length (mm)	Width (mm)	w and s (mm)	L (Sim.) ( $\mu\text{H}$ )	L (Meas.) ( $\mu\text{H}$ )	R (Meas.) ( $\Omega$ )	Q (Meas.)	NFC tag layout
1	6	44	44	1	1.83	$1.82 \pm 0.17$	$68.28 \pm 4.2$	$1.93 \pm 0.013$	
2	7	29	29	0.5	1.81	$1.78 \pm 0.11$	$46.32 \pm 3.5$	$2.13 \pm 0.011$	
3	7	26	26	0.4	1.79	$1.79 \pm 0.13$	$71.22 \pm 3.95$	$1.6 \pm 0.011$	
4	8	19	16	0.2	1.83	-	$124.53 \pm 5.1$	-	

( $C_{ext}$ ) of 39 pF and planar printed inductor of 1.8  $\mu$ H to decrease the size of the designed antenna.

$$f_{ref} = \frac{1}{\sqrt{2\pi L(C_{int}||C_{ext})}} \quad (1)$$

Four different inductor geometries have been considered (see **Table 1**) to find the optimised design in terms of quality factors. Inductors were simulated using the Advanced Design System (ADS) simulator (Keysight Technologies, Santa Clara, CA, USA). **Table 1** includes simulated values for inductors considering that the sheet resistance of the silver conducting paste is 95 m $\Omega$ /sq. These inductors were screen-printed using silver conductor paste (PE872) (Dupont, UK.) and characterised using an Agilent 4294A Precision Impedance Analyzer and a 42941A impedance probe kit fixture (Keysight Technologies, Santa Clara, CA, USA). A semi-automatic screen printer (model C920, Aurel Automation, Italy) was used to print inductors.

### B. Inductor Geometries

Table 1 summarizes the geometry and dimensions of the four designed inductors as well as simulated and measured values of the inductance. Here ‘w’ and ‘s’ stand for width and space between conductor tracks respectively. The resistance value of each layer of printed inductor and the quality factor are also included. The inductors were printed on matt photo paper (Rymans, UK.) and cured in oven at 90°C for 30 mins. The fourth design which has the tiniest track lines did not behave as an inductor with the predicted value. This could be due to the density of the tracks, meaning that 0.2 mm interspace between tracks is not the good even, although the simulation shows that it can create 1.83  $\mu$ H inductance. The overall resistance of the lines was also the highest, as was expected. Among the other three designs, the second one (see Fig. 1(a)) which was a square-shaped inductor with 29 mm length shows the highest quality factor, so we continued with this design and increased the number of printed layers to achieve the maximum quality factor. Fig. 1(b) shows the frequency response of this antenna before attaching the  $C_{ext}$  and the NFC transponder. A  $1.78 \pm 0.11 \mu$ H at 13.56 MHz was achieved, which is close to the simulated inductance value. The measured quality factor at the same frequency was  $Q = 2.13 \pm 0.071$ . Increasing the number of printed layers has improved the quality factor, as is shown in Fig. 1(c). Printing three layers has increased the quality factor to 4.73 and it was not practically possible to increase it further because adjacent tracks were merging. This effect is like the coffee effect in inkjet printing which leads to a new layer of printing spread slightly and the lines are wider compared to the previously printed layer. So, three printing layers of conductive ink were the optimum we could achieve.

### C. Optimised screen-printed NFC tag

The additive manufacturing based smart tag is shown in Fig. 2, which works in NFC ISO15693 communication technology (see supplementary video S1) This is our final screen-printed tag, designed after optimizing the antenna structure, substrate, and electrical bonding materials. The selection of suitable substrate and adhesive materials is discussed in the following sections.

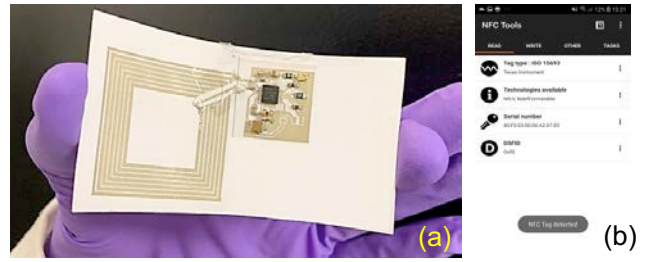


**Fig. 2.** (a) The NFC transponder-based screen-printed smart tag and (b) the detection of the tag by NFC enabled smartphone app named NFC Tool

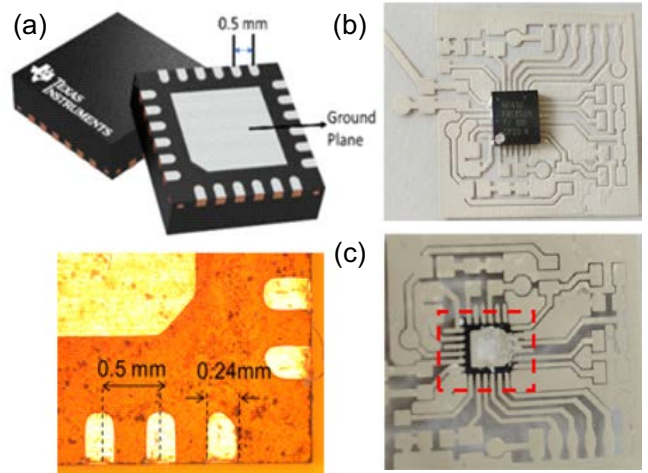


**Fig. 3.** The NFC transponder IC: (a) front and backside of the bare chip, (b) ground plane is mounted on the printed layer of the smart tag, and (c) spread of the silver paint after curing

**TABLE II:** VARIOUS POLYESTERS (PLASTICS) USED AS THE SUBSTRATE TO PRINT SMART TAGS.

Substrates	Max sustainable Temperature (°C)	Liner
Transfer PET white PT16	90	Glassine paper
Transfer white PET30	70	No
Gloss white PET	The liner shrinks at 60 and wrinkles appear on top	Kraft white paper

## III. CHALLENGES IN ELECTRICAL BONDING AND MECHANICAL STABILITY

In this section, suitable substrate materials are studied in detail along with the adhesives to highlight the challenges for particular application of VQFN chip-based screen-printed electronics.

### A. Polyester substrate with silver paste adhesive

Three polyester substrates of around 70  $\mu$ m thickness were chosen at first to screen print the designed circuit. Table 2 shows the difference in substrates according to their sustainable temperature and liner specifications. The NFC transponder RF430FRL152H is a VQFN packaged 24 pin tiny chip with the dimension of 4mm  $\times$  4mm and with a spacing of 0.25 mm between the two consecutive pins (Fig. 3(a)). Since this package has a high contact area compared to leaded surface mount components the mechanical robustness is higher when the chip is attached to the substrate. At first,

silver paint is used as the adhesive to bond the IC on the silver pattern. As the adhesive is in a semi-liquid state, small misalignment in the mounting process of the IC could result in an erroneous connection between the printed patterns.

To prevent this issue the ground plane (Fig. 3(b)) of the SMT component i.e. NFC transponder is mounted efficiently by depositing a little amount of conductive adhesive like silver paint with the help of a needle on the substrate, and thereafter cured at 80°C. However, the paint still spreads at the time of curing and makes an undesirable connection between the pads of the IC. Fig 3(c) shows the spread of the paint.

### B. Polyester substrate with silver epoxy adhesive

In order to overcome the issue of ink spreading, we considered silver-filled conductive epoxy as it is more viscous than silver paint. However, the electrical bonding of the pins of the VQFN-packaged IC with the adhesive is a big challenge as the pins are 0.25 mm apart. Because of closeness of the pins, they need to be connected to the printed pattern under the microscope. Manual deposition of the adhesive with a gap of 0.25 mm distance is extremely challenging. Even after the efficient deposition on the substrate as well as on the wall of the IC, deposition of the epoxy at the junction of the IC and the substrate is not fully achievable (Fig. 4(a)). Therefore, an arrangement was made (Fig. 4(b)) by fixing the substrate on a curvature to get a 45° angle view of the junction for the bonding at the junction but it failed as the epoxy is not solid. Additionally, the mechanical stability of the bonding with the conductive adhesive is a challenge. The small SMT (0603 packaged) parts like capacitors can be bonded strongly (Fig. 5), however, the electrical bonding with the IC is not robust enough to sustain the rough handling. The bending of the substrate can detach the IC from the printed pattern and may also damage the printed pattern permanently without the further possibility of bonding (Fig. 5).

### C. Polyimide substrate with low-temperature solder paste

The above-mentioned challenges could be overcome by using Sn42/Bi57.6/Ag0.4 low-temperature solder paste, where hot air at a temperature of 138°C is used to melt the solder paste to realise the electrical bonding. However, due to thermal budget issues this cannot be used with many non-conventional substrates that are used in flexible electronics. For example, the Polyester (70 mm) substrate cannot sustain in more than 80°C temperature. Therefore, we chose Polyimide substrate, which can sustain up to 400°C temperature. Whilst the substrates issues is resolved with Polyimide, we noted that at 138°C the printed silver patterns is removed (Fig. 6).

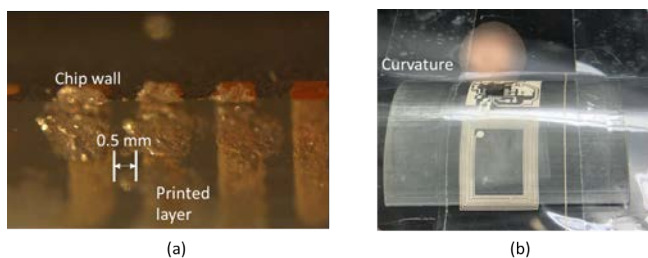


**Fig. 4.** (a) The silver epoxy is not present at the junction of chip wall and the printed layer, (b) A curvature arrangement to get a 45° view of the junction.

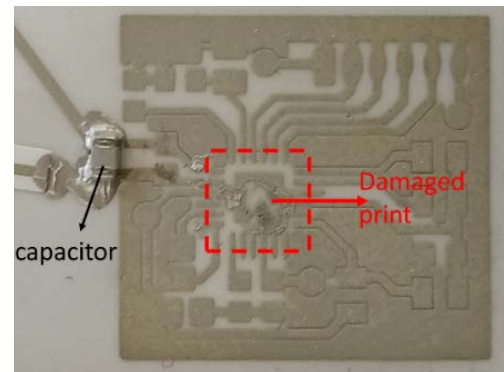


**Fig. 5.** Permanent damage of the printed layer due to the detachment of the IC

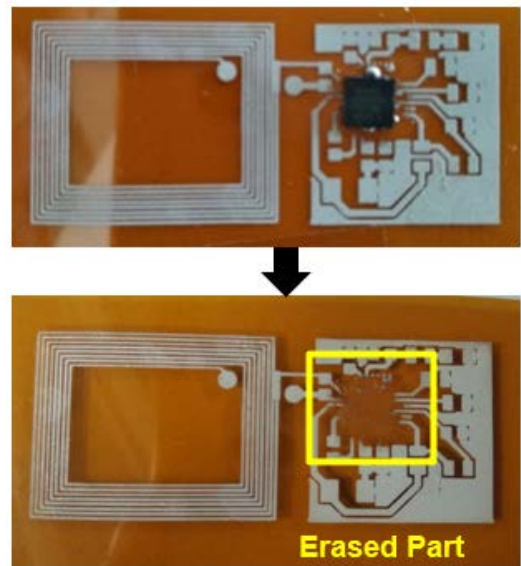


**Fig. 6.** Silver patterns are erased due to the temperature of the hot air gun on the glossy substrate

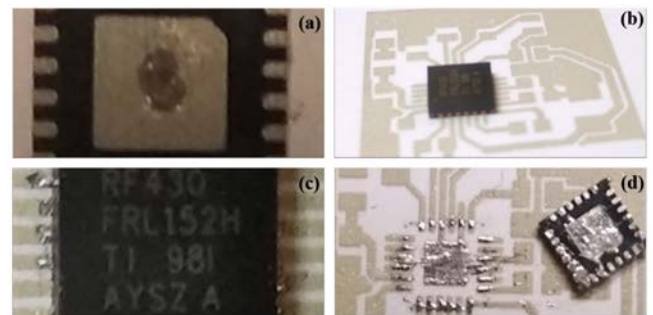


**Fig.7.** (a)-(c) Process of electrical bonding of IC in paper substrate, (d) Bonding failure

## IV. FLEXIBLE PAPER SUBSTRATE AS THE SOLUTION

The above challenges led us to the matt photopaper (240 gsm) substrate which can sustain the melting temperature of the solder paste. Relative dielectric permittivity of the selected photopaper is measured in the NFC frequency range of 13.56 MHz and it is found ~ 3.2 for this substrate. Additionally, paper is one of the biodegradable materials and can help in reducing e-waste. Solder paste had the strong mechanical stability of the IC with the photopaper. In this process, solder paste is added on the ground plane of the IC

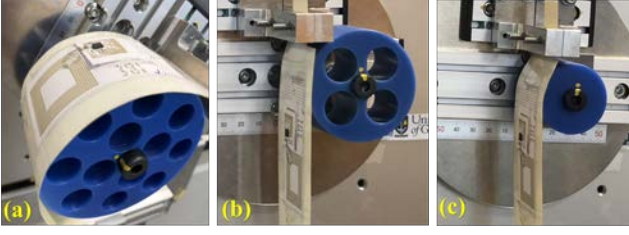


**Fig. 8.** (a)-(c) The smart tag is projected to the bending condition of 40 mm, 30 mm, and 20 mm of radius.

(Fig. 7(a)), then IC is aligned precisely, and hot air is blown over it at 140°C temperature. Once the ground plane is fixed, a little solder paste is applied uniformly on each side of the square IC (Fig. 7 (b)) and there is no need for application of solder paste to each pin of the IC. Because of the hot air, the solder only makes the bonding with the silver tracks, not with the paper substrate and this minimizes the probability of shorting consecutive pins of the tiny IC. The complete soldered IC is shown in Fig. 7 (c). However, the hot air should be blown perpendicular to the IC, otherwise the chip shifts its place and may make an unwanted connection between the tracks (Fig. 7 (d)). It is worth mentioning that paper substrate in the RFID tag is used in few works reported in literature [18, 19], however, integration of VQFN chip and the challenges related to connecting consecutive pins of the chip are not discussed before.

### A. Mechanical reliability testing

A stress test is performed with different bending radii to determine the sustainable level of bending for the tag. A bending and twisting endurance setup (Yuasa DMLHP) is used for this measurement. We have started from the bending condition of 40 mm radius and gradually reduced the radius by 10 mm (see supplementary video S2). In each bending condition, 10 cyclic rotations are performed, and NFC enabled smartphone is used to check the detectability of the tag. The tag works perfectly for the bending radius of 40 mm and 30 mm, however, after the 10 cyclic rotations in 20 mm radius, the tag is not detectable anymore as pin 2 of the NFC transponder is no longer attached with the printed circuit which leads to the loss of the electrical connection. The experimental photograph with 40 mm, 30 mm, and 20 mm radius of bending is shown in Fig. 8(a), (b), and (c) respectively.

## V. ANTENNA CHARACTERISATION

This section describes the characterisation of the final photopaper based smart tag. In the near field configuration, the communication takes place when a reader passes a large alternating current through a reading coil, thus, resulting in creation of local alternating magnetic field (see Fig. 9(a)). When the near field tag is placed in the vicinity of the generated magnetic field of the reader, an alternating voltage will appear across the inductive loop antenna of the tag [22]. This voltage is first rectified in the energy harvester unit of

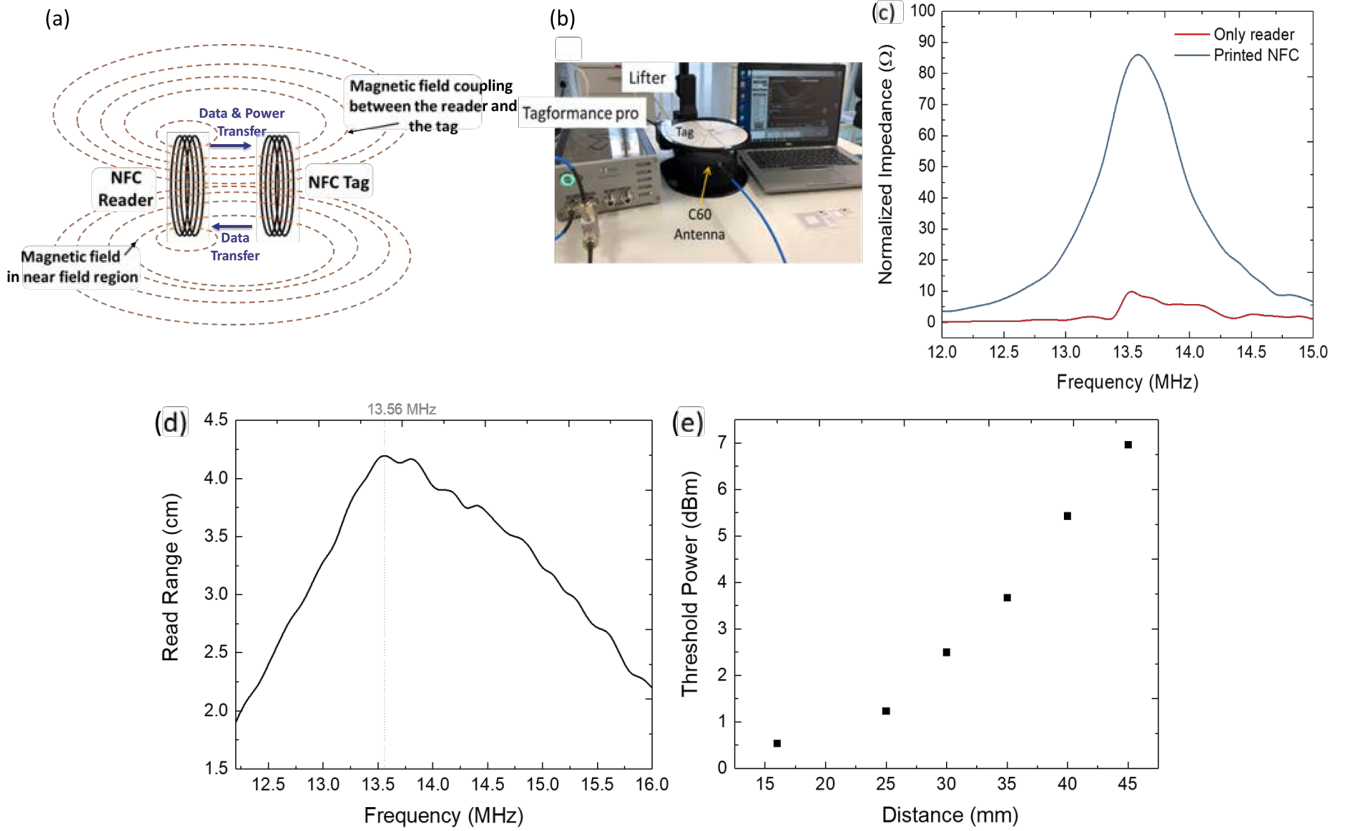


**Fig. 9.** (a) Schematic of Near-field inductive coupling for power and data transmission (b) Voyantic Setup for characterisation of NFC tags. (c) The input impedance of the reader antenna is measured with and without presenting the tag in its proximity. The peak impedance at 13.6 MHz is very close to 13.56 MHz, which is the frequency the tag was designed for. (d) Change in reading range function of the frequency sweep. The distance was kept constant (16 mm). (e) Output power as function of distance from the reader.

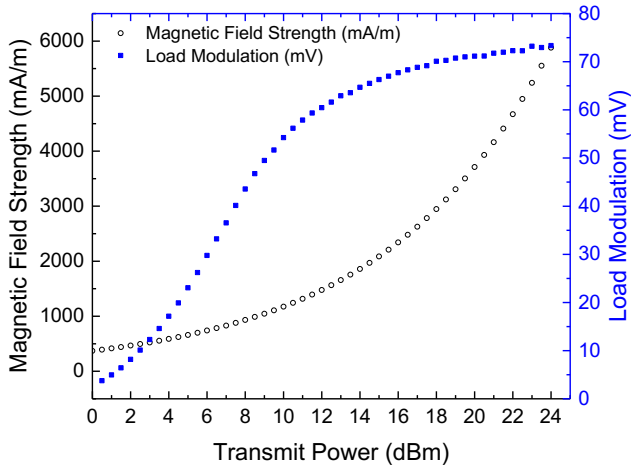


**Fig. 10.** Threshold power of the printed tag as a function of magnetic field intensity and load modulation at 13.56 MHz

the tag to power the electronics of the tag chip. Also, the demodulation of the interrogation signal is achieved to get the interrogation information. RFID Tags based on near-field coupling send the data back to the reader using load modulation [23]. The load modulation generates a current variation proportional to the load applied to the tag's coil giving rise to its own small magnetic field which will oppose the reader's field and therefore the reader coil can detect data as a small variation in current. This signal encoded as tiny variation in the magnetic field strength represents the tag's identification (ID) [24]. The reader can then recover this signal by monitoring the change in current through the reader coil. A variety of modulation encoding is possible depending on the number of ID bits required, the data transfer rate, and additional redundancy bits placed in the code to remove errors that result from communication channel noise. Near-field coupling is the most straightforward approach for implementing a passive RFID system. This is why it was the first adopted approach and has resulted in many subsequent standards, such as ISO 15693 and 14443, and a variety of proprietary solutions [25].

Tagformance Pro HF is used to characterise the paper-based printed NFC tag as shown in Fig. 9(b). The equipment works similar to a vector network analyser to measure the effect of the designed NFC tag on the input impedance of a reader antenna. The reader antenna was a Voyantic C60 antenna which is a loop (diameter 60 mm) antenna with 4 turns. The input impedance of the reader antenna is measured with and without the presence of the tag in its proximity (see Fig. 9(c)). The peak of impedance occurred at 13.6 MHz, which is very close to 13.56 MHz - the frequency the tag was designed for. The reading range of the tag is shown in Fig. 8(d) when the output power of the reader is set 0 dBm. The maximum reading range of the printed tag is about 4.2 cm.

The threshold power ( $P_{th}$ ) was measured to evaluate the sensitivity of the tag with distance from the reader antenna. In this regard, the tag was placed on the lifter (see Fig. 9(d)) to adjust the measurement distance. During this measurement, the tag interrogates with the reader while the distance between the tag and the reader was increased from 16 mm to 45 mm. As shown in Fig. 9(e), the threshold power increases as the lifter goes up. The initial output power was 0 dBm and frequency was swept from 10 MHz to 20 MHz with 10 kHz resolution. The lowest output power in each distance was

noted at 13.6 MHz, which is the optimal operating frequency of the tag. In the case that an NFC-enabled smartphone is used as the reader the power that the phone can provide to this unit defined the reading range of the tag.

The data of the transponder RFIC is sent back via RF signal in a process called load modulation. Load modulation takes place in the alternation of the antenna load, which leads to a change of the backscattered signal. Fig. 10 shows the relation between the variation in  $P_{th}$  and the load modulation of the printed tag at 13.56 MHz at a 16 mm distance from the reader. It shows the threshold of the transmitted power to have the strongest modulation. The load modulation also is a function of magnetic field intensity (see Fig. 9) of the tag to evaluate the tag performance on all power levels to find the optimal power level to communicate with the tag.

## VI. CONCLUSION

The mechanical stability of electronic components and appropriate electrical contacts on the printed substrates are necessary for the development of robust flexible electronics. In this regard, hybrid integration of microchips on printed tags has been explored here. Four inductors were designed to examine the effect of the number of turns and dimensions on the quality factor of the screen-printed NFC tag. The effect of number of printed layers to achieve optimum quality factor is studied. The quality factor of 4.73 is achieved by increasing the number of printed layers to three. Moreover, connection strategies of VQFN-packaged NFC transponder on four different commercially available substrates are analysed and photopaper is shown as the suitable substrate for connecting the IC with low-temperature solder paste. The results demonstrate that the reading range of 4.2 cm is feasible for the reader output power of 0 dBm. The results lead to the conclusion that the hybrid integration is a promising approach to fabricate low-cost and environmentally friendly paper-based NFC tags and that there is need to explore more solutions for bonding and packaging.

## ACKNOWLEDGEMENTS

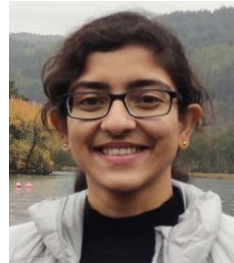
This work was supported by North West Centre for Advanced Manufacturing (NWCAM) project, supported by the European Union's INTERREG VA Programme (H2020-Intereg-IVA5055), managed by the Special EU Programmes Body (SEUPB). The views and opinions in this document do not necessarily reflect those of SEUPB.

## REFERENCES

- [1] S. Ma, Y. Kumaresan, A. S. Dahiya, and R. Dahiya, "Ultra - Thin Chips with Printed Interconnects on Flexible Foils," *Advanced Electronic Materials*, p. 2101029, 2021.
- [2] C. Song *et al.*, "Advances in Wirelessly Powered Backscatter Communications: From Antenna/RF Circuitry Design to Printed Flexible Electronics," *Proceedings of the IEEE*, vol. 110, no. 1, pp. 171-192, 2021.
- [3] R. Bhattacharyya, C. Floerkemeier, and S. Sarma, "Low-cost, ubiquitous RFID-tag-antenna-based sensing," *Proceedings of the IEEE*, vol. 98, no. 9, pp. 1593-1600, 2010.
- [4] C. Occhiuzzi, S. Parrella, F. Camera, S. Nappi, and G. Marrocco, "RFID-based dual-chip epidermal sensing platform for human skin monitoring," *IEEE Sensors Journal*, vol. 21, no. 4, pp. 5359-5367, 2020.
- [5] S. Khan, L. Lorenzelli, and R. S. Dahiya, "Technologies for printing sensors and electronics over large flexible substrates: a review," *IEEE Sensors Journal*, vol. 15, no. 6, pp. 3164-3185, 2014.

- [6] G. A. T. Sevilla and M. M. Hussain, "Printed organic and inorganic electronics: Devices to systems," *IEEE Journal on Emerging and Selected Topics in Circuits and Systems*, vol. 7, no. 1, pp. 147-160, 2016.
- [7] S. Kim, A. Georgiadis, and M. M. Tentzeris, "Design of inkjet-printed RFID-based sensor on paper: Single-and dual-tag sensor topologies," *Sensors*, vol. 18, no. 6, p. 1958, 2018.
- [8] F. Nikbakhtnasrabadi, E. S. Hosseini, S. Dervin, D. Shakthivel, and R. Dahiya, "Smart bandage with inductor-capacitor resonant tank based printed wireless pressure sensor on electrospun Poly-L-lactide nanofibers," *Advanced Electronic Materials*, p. 2101348, 2022.
- [9] P. Escobedo, M. Bhattacharjee, F. Nikbakhtnasrabadi, and R. Dahiya, "Flexible Strain and Temperature Sensing NFC Tag for Smart Food Packaging Applications," *IEEE Sensors Journal*, vol. 21, no. 23, pp. 26406-26414, 2021.
- [10] F. Nikbakhtnasrabadi, H. El Matbouly, M. Ntagios, and R. Dahiya, "Textile-Based Stretchable Microstrip Antenna with Intrinsic Strain Sensing," *ACS Applied Electronic Materials*, vol. 3, no. 5, pp. 2233-2246, 2021.
- [11] P. Escobedo, M. Bhattacharjee, F. Nikbakhtnasrabadi, and R. Dahiya, "Smart Bandage With Wireless Strain and Temperature Sensors and Batteryless NFC Tag," *IEEE Internet of Things Journal*, vol. 8, no. 6, pp. 5093-5100, 2020.
- [12] M. Bhattacharjee, F. Nikbakhtnasrabadi, and R. Dahiya, "Printed Chipless Antenna as Flexible Temperature Sensor," *IEEE Internet of Things Journal*, vol. 8, no. 6, pp. 5101-5110, 2021.
- [13] L. Rauter, J. Zikulnig, T. Sinani, H. Zangl, and L.-M. Fallner, "Evaluation of Standard Electrical Bonding Strategies for the Hybrid Integration of Inkjet-Printed Electronics," *Electronic Materials*, vol. 1, no. 1, pp. 2-16, 2020.
- [14] M. Bhattacharjee, S. Middy, P. Escobedo, J. Chaudhuri, D. Bandyopadhyay, and R. Dahiya, "Microdroplet based disposable sensor patch for detection of  $\alpha$ -amylase in human blood serum," *Biosensors and Bioelectronics*, vol. 165, p. 112333, 2020.
- [15] K. Sima, T. Syrový, S. Pretl, J. Freisleben, D. Cesek, and A. Hamacek, "Flexible smart tag for cold chain temperature monitoring," in *2017 40th International Spring Seminar on Electronics Technology (ISSE)*, 2017: IEEE, pp. 1-5.
- [16] X. Zhang, X. Shan, and J. Wei, "Hybrid flexible smart temperature tag with NFC technology for smart packaging," in *2017 IEEE 19th Electronics Packaging Technology Conference (EPTC)*, 2017: IEEE, pp. 1-5.
- [17] E. Balliu, H. Andersson, M. Engholm, T. Öhlund, H.-E. Nilsson, and H. Olin, "Selective laser sintering of inkjet-printed silver nanoparticle inks on paper substrates to achieve highly conductive patterns," *Scientific reports*, vol. 8, no. 1, pp. 1-9, 2018.
- [18] M. M. Tentzeris, A. Rida, A. Traill, H. Lee, V. Lakafosis, and R. Vyas, "Inkjet-printed paper/polymer-based RFID and Wireless Sensor Nodes: The final step to bridge cognitive intelligence, nanotechnology and RF?," in *2011 XXXth URSI General Assembly and Scientific Symposium*, 2011: IEEE, pp. 1-4.
- [19] H. Andersson, J. Sidén, V. Skerved, X. Li, and L. Gyllner, "Soldering surface mount components onto inkjet printed conductors on paper substrate using industrial processes," *IEEE Transactions on Components, Packaging and Manufacturing Technology*, vol. 6, no. 3, pp. 478-485, 2016.
- [20] H. Nassar and R. Dahiya, "Fused Deposition Modeling - Based 3D - Printed Electrical Interconnects and Circuits," *Advanced Intelligent Systems*, vol. 3, no. 12, p. 2100102, 2021.
- [21] K. Finkenzeller, *RFID handbook: fundamentals and applications in contactless smart cards, radio frequency identification and near-field communication*. John Wiley & sons, 2010.
- [22] A. Rahul, S. Rao, and M. Raghu, "Near field communication (NFC) technology: a survey," *International Journal on Cybernetics & Informatics (IJCI)*, vol. 4, no. 2, p. 133, 2015.

- [23] H. A. Al-Ofeishat and M. A. Al Rababah, "Near field communication (NFC)," *International Journal of Computer Science and Network Security (IJCSNS)*, vol. 12, no. 2, p. 93, 2012.
- [24] T. A. Martins, J. Saldaña, and W. Van Noije, "A Programmable Gain Amplifier for Load Demodulation Channel in an NFC Reader Chip," in *2018 31st Symposium on Integrated Circuits and Systems Design (SBCCI)*, 2018: IEEE, pp. 1-6.
- [25] I.-F. Chen, C.-M. Peng, and Z.-D. Yan, "A simple NFC parameters measurement method based on ISO/IEC 14443 standard," in *2019 IEEE International Conference on RFID Technology and Applications (RFID-TA)*, 2019: IEEE, pp. 33-36.



**Moupali Chakraborty** (S'16-M'21) received B.Tech in Electronics & Instrumentation Engineering in 2010, and M.Tech in Instrumentation Engineering in 2015, followed by a PhD in Electrical Engineering from IIT Kharagpur, India in 2020 with the specialization in Instrumentation system.

From 2011 to 2013 she worked as a System Engineer in Tata Consultancy services. Since April 2021, she is working as a Postdoctoral Researcher in Bendable Electronics and Sensing Technology (BEST) group of the department of Electronics & Nanoscale Engineering at University of Glasgow, United Kingdom. Her current research interest includes design of interfacing circuit, flexible and printed electronics, development of instrumentation system, and device characterization.



**Fatemeh Nikbakhtnasrabadi** (S'18) received the B.Sc. Degree in Electrical Engineering in 2010 and MSc. in Telecommunication Engineering in 2013 from Shahed University, Tehran, Iran. Currently, she is pursuing PhD degree in the Electronics and Nanoscale Division with Bendable Electronics and Sensing Technologies Group at the University of Glasgow, UK. Her current research interest includes the development of flexible electronic, sensing antenna and printed RFID for healthcare monitoring and smart labels.



**Ravinder Dahiya** (Fellow, IEEE) is Professor of Electronics and Nanoengineering in the University of Glasgow, U.K. He is the leader of Bendable Electronics and Sensing Technologies (BEST) research group. His group conducts fundamental and applied research in flexible and printable electronics, tactile sensing, electronic skin, robotics, and wearable systems. He has authored over 400 research articles, 8 books, and 15 submitted/granted patents. He has led several international projects. He is President-Elect (2020-21) and Distinguished Lecturer of the IEEE Sensors Council. He is the Founding Editor in Chief of IEEE JOURNAL ON FLEXIBLE ELECTRONICS and has served on the editorial boards of the Scientific Report, IEEE SENSORS JOURNAL (2012-2020) and IEEE TRANSACTIONS ON ROBOTICS (2012-2017). He was the Technical Program co-chair of IEEE Sensors 2017 and IEEE Sensors 2018 and has been General Chair of several conferences including IEEE FLEPS (2019, 2020, 2021), which he founded in 2019. He holds the prestigious EPSRC Fellowship and received in past the Marie Curie and Japanese Monbusho Fellowships. He has received several awards, including 2016 Microelectronic Engineering Young Investigator Award (Elsevier), 2016 Technical Achievement Award from the IEEE Sensors Council and 11 best paper awards as author/coauthor in International Conferences and Journals.



